

# Efficient solutions of self-consistent mean field equations for dewetting and electrostatics in nonuniform liquids

Zhonghan Hu\* and John D. Weeks

*Institute for Physical Science and Technology and Department of Chemistry and Biochemistry,  
University of Maryland, College Park, Maryland 20742*

(Dated: September 17, 2010)

We use a new configuration-based version of linear response theory to efficiently solve self-consistent mean field equations relating an effective single particle potential to the induced density. The versatility and accuracy of the method is illustrated by applications to dewetting of a hard sphere solute in a Lennard-Jones fluid, the interplay between local hydrogen bond structure and electrostatics for water confined between two hydrophobic walls, and to ion pairing in ionic solutions. Simulation time has been reduced by more than an order of magnitude over previous methods.

Mean field theories have long provided a physically suggestive and qualitatively useful description of structure, thermodynamics, and phase transitions in condensed matter systems. In these approaches certain long-ranged components of the intermolecular interactions are replaced by an effective single particle potential or “molecular field” that depends self-consistently on the nonuniform density the field itself induces [1]. Recent work has shown that this method can produce exceptionally accurate results for models of simple and molecular liquids, ionic fluids, and water provided that i) all the intermolecular interactions averaged over are slowly varying at typical nearest neighbor distances where strong local forces dominate and ii) an accurate description of the density induced by the effective field is used [2–5]. When both these conditions are satisfied we call the resulting approach Local Molecular Field (LMF) theory.

LMF theory can be viewed as a mapping that relates the structure and thermodynamics of the full long-ranged system to those of a simpler “mimic system” with truncated intermolecular interactions but in an effective or restructured field that accounts for the averaged effects of the long-ranged interactions [2, 3]. Analyzing the short-ranged mimic system may offer particular advantages for systems with Coulomb interactions, since standard particle-mesh Ewald sum treatments do not scale well in massively-parallel simulations [6]. But to realize the full potential of LMF theory as a practical tool in computer simulations and in qualitative analysis, we must efficiently determine the effective field. We show here that when condition i) above is satisfied we can use a new configuration-based version of linear response theory to satisfy condition ii) as well. This leads to a highly accurate and efficient way to solve the self-consistent LMF equation. These ideas may also help solve self-consistent-field equations that appear in many other contexts.

To illustrate the method in its simplest form, we first study dewetting of a single hard sphere “solute” particle in a Lennard-Jones (LJ) fluid. However LMF theory provides a unified perspective and only minor changes are needed to describe more complex systems with Coulomb interactions. Here we focus on the coupling between

dewetting and electrostatics in water confined by hydrophobic walls and on ion pairing in ionic solutions. Long-ranged forces play a key but subtle role in all these examples and require a very accurate solution of the LMF equation.

Consider a nonuniform LJ fluid in the presence of the field  $\phi_0(\mathbf{r})$  generated by the hard sphere solute, as described below. The LJ pair potential is separated by the sign of the force into a short-ranged repulsive core and a longer-ranged perturbation part [7]:  $u_{LJ}(r_{ij}) = u_0(r_{ij}) + u_1(r_{ij})$ .  $u_1$  contains only slowly-varying attractive forces and thus is suitable for LMF averaging. The LJ mimic system has truncated intermolecular interactions  $u_0(r_{ij})$  in the presence of an effective or restructured field  $\phi_R(\mathbf{r})$ , chosen in principle so that the nonuniform density  $\rho_R(\mathbf{r}; [\phi_R]) \equiv \langle \rho(\mathbf{r}, \bar{\mathbf{R}}) \rangle_{\phi_R}$  in the mimic system (indicated by the subscript R) equals the density  $\rho(\mathbf{r}; [\phi_0])$  in the full system [2–5]. Here  $\langle \rangle_{\phi_R}$  denotes a normalized ensemble average in the mimic system in the presence of  $\phi_R$ ,  $\bar{\mathbf{R}} \equiv \{\mathbf{r}_i\}$  denotes a microscopic configuration of all particles, and  $\rho(\mathbf{r}, \bar{\mathbf{R}}) \equiv \sum_{i=1}^N \delta(\mathbf{r} - \mathbf{r}_i)$  is the microscopic configurational density.

As shown in detail elsewhere [2–5],  $\phi_R$  and the associated equilibrium density  $\rho_R(\mathbf{r}; [\phi_R])$  can be accurately determined by solving the self-consistent LMF equation

$$\phi_R(\mathbf{r}) = \phi_0(\mathbf{r}) + \int d\mathbf{r}' \rho_R(\mathbf{r}'; [\phi_R]) u_1(|\mathbf{r} - \mathbf{r}'|) + C, \quad (1)$$

where  $C$  is a constant setting the zero of energy [8].

In earlier work [4, 5], the LMF equation was solved by straightforward iteration, using computer simulations to accurately determine the density induced by the given field at each iteration. However, even with a good initial estimate  $\tilde{\phi}_0$  for the effective field, determining the density induced by the remaining changes in the field  $\tilde{\phi}_{R1} \equiv \phi_R - \tilde{\phi}_0$  from further iterations required more simulations. By rewriting the density in Eq. (1) so that the dependence on  $\tilde{\phi}_{R1}$  appears inside the ensemble average, we show here that the LMF equation can be iterated to self-consistency with no new simulations required.

This is very easy to do formally. We refer to the system with effective field  $\tilde{\phi}_0$  as a “trial” system and note that

the total potential energy associated with the correction  $\tilde{\phi}_{R1}$  in a configuration  $\bar{\mathbf{R}}$  is given by

$$\tilde{\Phi}_{R1}(\bar{\mathbf{R}}) \equiv \sum_{i=1}^N \tilde{\phi}_{R1}(\mathbf{r}_i) = \int d\mathbf{r} \rho(\mathbf{r}, \bar{\mathbf{R}}) \tilde{\phi}_{R1}(\mathbf{r}). \quad (2)$$

Similarly defining  $U_0(\bar{\mathbf{R}})$  as the total intermolecular potential energy in configuration  $\bar{\mathbf{R}}$  we have exactly

$$\begin{aligned} \langle \rho(\mathbf{r}, \bar{\mathbf{R}}) \rangle_{\phi_R} &= \frac{\int d\bar{\mathbf{R}} \rho(\mathbf{r}, \bar{\mathbf{R}}) e^{-\beta[U_0(\bar{\mathbf{R}}) + \tilde{\Phi}_0(\bar{\mathbf{R}}) + \tilde{\Phi}_{R1}(\bar{\mathbf{R}})]}}{\int d\bar{\mathbf{R}} e^{-\beta[U_0(\bar{\mathbf{R}}) + \tilde{\Phi}_0(\bar{\mathbf{R}}) + \tilde{\Phi}_{R1}(\bar{\mathbf{R}})]}} \\ &= \frac{\langle \rho(\mathbf{r}, \bar{\mathbf{R}}) e^{-\beta \tilde{\Phi}_{R1}(\bar{\mathbf{R}})} \rangle_{\tilde{\phi}_0}}{\langle e^{-\beta \tilde{\Phi}_{R1}(\bar{\mathbf{R}})} \rangle_{\tilde{\phi}_0}}. \end{aligned} \quad (3)$$

The idea behind Eq. (3), usually with a configuration dependent function  $F(\bar{\mathbf{R}})$  replacing  $\rho(\mathbf{r}, \bar{\mathbf{R}})$  and different choices of trial and full systems, is very well known and serves as the basis for perturbation and weighted histogram methods for thermodynamic properties [9]. Here we use it to determine changes of the density in the LMF equation as the iteration proceeds to self-consistency.

Averaging over exponentials as in Eq. (3) is usually problematic, and in most applications sophisticated techniques like umbrella sampling are needed to obtain good statistics [9]. However, condition i), required for the quantitative validity of LMF theory itself, ensures that only slowly varying intermolecular forces appear in  $\tilde{\Phi}_{R1}(\bar{\mathbf{R}})$ . This suggests it may not be difficult to find a trial field  $\tilde{\phi}_0$  for which the exponential remainder  $e^{-\beta \tilde{\Phi}_{R1}(\bar{\mathbf{R}})}$  varies sufficiently slowly over most relevant configurations  $\bar{\mathbf{R}}$  that a simple direct average is accurate.

A linearization of Eq. (3) provides a way to test for this condition. Defining  $\delta\tilde{\Phi}_{R1}(\bar{\mathbf{R}}) \equiv \tilde{\Phi}_{R1}(\bar{\mathbf{R}}) - \langle \tilde{\Phi}_{R1}(\bar{\mathbf{R}}) \rangle_{\tilde{\phi}_0}$  and  $\delta\rho(\mathbf{r}, \bar{\mathbf{R}}) \equiv \rho(\mathbf{r}, \bar{\mathbf{R}}) - \langle \rho(\mathbf{r}, \bar{\mathbf{R}}) \rangle_{\tilde{\phi}_0}$ , we find

$$\langle \rho(\mathbf{r}, \bar{\mathbf{R}}) \rangle_{\phi_R} \simeq \langle \rho(\mathbf{r}, \bar{\mathbf{R}}) \rangle_{\tilde{\phi}_0} - \beta \langle \delta\rho(\mathbf{r}, \bar{\mathbf{R}}) \delta\tilde{\Phi}_{R1}(\bar{\mathbf{R}}) \rangle_{\tilde{\phi}_0}. \quad (4)$$

This is equivalent to the usual linear response formula

$$\begin{aligned} \langle \rho(\mathbf{r}, \bar{\mathbf{R}}) \rangle_{\phi_R} &\simeq \langle \rho(\mathbf{r}, \bar{\mathbf{R}}) \rangle_{\tilde{\phi}_0} \\ &- \beta \int d\mathbf{r}' \langle \delta\rho(\mathbf{r}, \bar{\mathbf{R}}) \delta\rho(\mathbf{r}', \bar{\mathbf{R}}) \rangle_{\tilde{\phi}_0} \tilde{\phi}_{R1}(\mathbf{r}') \end{aligned} \quad (5)$$

on using Eq. (2). However the linear response (LR) function  $\langle \delta\rho(\mathbf{r}, \bar{\mathbf{R}}) \delta\rho(\mathbf{r}', \bar{\mathbf{R}}) \rangle_{\tilde{\phi}_0}$  depends on  $\mathbf{r}$  and  $\mathbf{r}'$  separately in a nonuniform system and is usually too complicated to be determined directly. In contrast, the averages in Eqs. (4) and (3) simply reweight the bin histograms used to determine the nonuniform density and depend on  $\mathbf{r}$  alone. They can be easily calculated using the saved configurations of a single well-chosen trial system.

For very slowly varying  $\tilde{\Phi}_{R1}(\bar{\mathbf{R}})$ , the system is in a linear regime where essentially identical structural changes

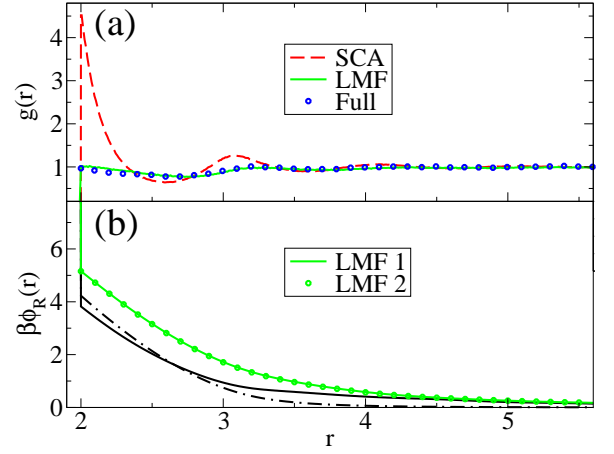


FIG. 1. LMF/LR/EXP treatment of the drying transition induced by a hard sphere solute in a LJ fluid for  $T = 0.85$ ,  $\rho^B = 0.70$ . (a) The RDF around a hard sphere cavity with  $R_c = 2$  for the full LJ fluid, the SCA trial system, and the converged LMF system. (b) Trial fields in the linear regime (solid and dot-dashed curves) and the final self-consistent field (circles and solid line) [11].

arise from the exponential (EXP) form in Eq. (3) or the LR form in Eq. (4). By requiring that a trial system gives the same result on iterating the LMF equation using both forms, we have a conservative and objective test for an accurate solution. We refer to this as the LR-LMF method, since in general Eq. (4) proves most useful. To our knowledge, the advantages of the configuration-based LR formula in Eq. (4) have not been exploited before.

We first study a hard sphere solute in a LJ fluid at a state near the triple point [10]. The solute is represented by an external field  $\phi_0(r)$  that is infinite inside a cavity of radius  $R_c$  and zero otherwise. In the simplest “strong coupling approximation” (SCA) to LMF theory, often successfully used in perturbation theories of uniform liquids [7], all effects of the slowly varying  $u_1$  on the molecular structure are ignored and the effective field  $\phi_R(r)$  is approximated by the bare hard sphere field  $\phi_0(r)$ . When  $R_c$  (measured in units of  $\sigma_{LJ}$ ) is unity, attractive forces nearly cancel and the SCA gives good results, correctly predicting an oscillatory density response with a large density maximum at contact.

However, as the cavity radius increases, particles near the cavity experience unbalanced attractive forces from LJ particles further away that reduce the contact density. Strong reduction already is seen for  $R_c = 2$ . The circles in Fig. 1a give results of computer simulations [11] for the radial distribution function (RDF)  $g(r; [\phi_0]) \equiv \rho(r; [\phi_0])/\rho^B$  induced by the hard sphere solute in the full LJ fluid with bulk density  $\rho^B$ . This exhibits an essentially structureless profile with a contact value of unity. The solid curve in Fig. 1a gives  $g_R(r; [\phi_R])$ , the RDF in the mimic system. The excellent agreement

between the LMF prediction and the full LJ  $g(r; [\phi_0])$  shows that LMF theory quantitatively captures the drying effect. This contrasts with the dashed line in Fig. 1a, the density in the truncated system induced by the bare field  $\phi_0$ . The failure of this SCA prediction illustrates the general need in most nonuniform systems for a proper self-consistent solution of the LMF equation.

The self-consistent field  $\phi_R(r)$  was obtained from solving Eq. (1) using two different trial fields shown in Fig. 1b. Both trial systems are in the linear regime and give the same final result. The solid curve results from a previous trial simulation based on the SCA that used the bare  $\phi_0(r)$ . As Fig. 1a suggests, this represents a very poor initial guess, and the EXP form (3) produced very noisy data, indicating poor overlap between the SCA and final LMF configurations. However Eq. (4) gave much smoother data and its use in the LMF equation gave the solid curve in Fig. 1b as the output field. Using this as a second trial field generates a converged solution of the LMF equation using either Eqs. (4) or (3).

Since  $u_1$  is slowly-varying, using relatively crude approximations to the asymmetric density in the LMF equation can often give a better trial field than the simple SCA. Thus in Fig. 1b, the dot-dashed trial field was found by approximating the density by a step function that vanishes inside the cavity and equals  $\rho^B$  outside.

LMF theory proves even more useful [4, 5] when applied to systems with Coulomb interactions in the presence of an electrostatic potential  $\mathcal{V}(\mathbf{r})$  arising from a fixed external charge distribution  $\rho_{\text{ext}}^q(\mathbf{r}')$ . The basic Coulomb interaction  $1/r \equiv v_0(r) + v_1(r)$  is separated into short- and long-ranged components, where  $v_1(r)$  is proportional to the electrostatic potential arising from a normalized Gaussian charge distribution with width  $\sigma$ ,

$$v_1(r) \equiv \frac{1}{\pi^{3/2}\sigma^3} \int e^{-r'^2/\sigma^2} \frac{1}{|\mathbf{r} - \mathbf{r}'|} d\mathbf{r}' = \frac{\text{erf}(r/\sigma)}{r}. \quad (6)$$

An advantage of the Coulomb separation is that  $\sigma$  can be chosen specifically in different applications so that condition i) is very well satisfied.

When all charges in the system (both fixed and mobile) are separated using the same  $\sigma$  and all other intermolecular interactions remain unchanged, LMF theory then gives a mapping to a Coulomb mimic system where all  $1/r$  interactions are replaced by the short-ranged  $v_0(r)$  and there is a restructured electrostatic potential  $\mathcal{V}_R$  that satisfies the Coulomb LMF equation

$$\mathcal{V}_R(\mathbf{r}) = \mathcal{V}_0(\mathbf{r}) + \int d\mathbf{r}' \rho_{R,\text{tot}}^q(\mathbf{r}'; [\mathcal{V}_R]) v_1(|\mathbf{r} - \mathbf{r}'|) + C. \quad (7)$$

Here  $\mathcal{V}_0(\mathbf{r})$  is the short-ranged part of the external potential, given by the convolution of  $v_0(r)$  with the fixed charge density, and  $\rho_{R,\text{tot}}^q(\mathbf{r}'; [\mathcal{V}_R])$  is the total equilibrium charge density from both fixed and mobile charges. An alternate form of Eq. (7) better relates LMF the-

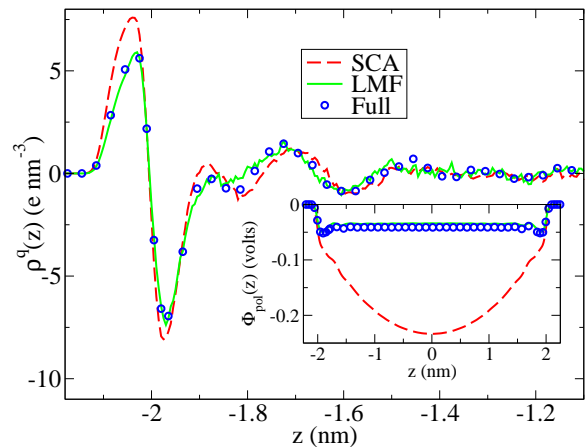


FIG. 2. Charge densities for water confined by hydrophobic LJ walls [13] centered at  $z = \pm 2.25$  nm for the SCA (dashed line), mimic system (solid line) and full system (circles). The inset shows the corresponding polarization potentials [11].

ory to conventional electrostatics [5]. Noting the convolution defining  $v_1$ , we see that the slowly-varying part  $\mathcal{V}_{R1}(\mathbf{r}) \equiv \mathcal{V}_R(\mathbf{r}) - \mathcal{V}_0(\mathbf{r})$  of the restructured potential in (7) exactly satisfies Poisson's equation but with a Gaussian-smoothed charge density  $\rho_{R,\text{tot}}^{q\sigma}$ , given by the convolution of  $\rho_{R,\text{tot}}^q$  with the Gaussian in Eq. (6).

We now apply the Coulomb LMF Eq. (7) to the extended simple point charge (SPC/E) model for water [12]. As suggested by the SCA, we first consider a Gaussian-truncated (GT) model, where all the  $1/r$  interactions from charges in SPC/E water are replaced by  $v_0(r)$  and we ignore all structural effects from  $v_1$ . Bulk GT water with  $\sigma = 0.45$  nm gives excellent results for both atom-atom and dipole-angle correlation functions when compared to the full SPC/E model, with Coulomb interactions treated by Ewald sums [5].

Moreover, as Fig. 2 shows, when GT water is confined between two hydrophobic LJ walls as defined in [13], the charge density  $\rho_0^q(z)$  determined by simulations [11] using bare wall fields with  $\mathcal{V}_0 = 0$  seems to capture most qualitative features of the dipole layer, a characteristic property of water near extended hydrophobic interfaces [5, 13]. Only small differences in the peak heights are visible when compared with full SPC/E water, simulated using the slab-corrected Ewald 3D method [14].

Nevertheless, as has long been recognized [15, 16], major errors are seen in the polarization potential felt by a test charge, given by integrating Poisson's equation:

$$\Phi_{\text{pol}}(z) = - \int_{-L/2}^z dz' \int_{-L/2}^{z'} dz'' \rho^q(z''). \quad (8)$$

As shown in the inset of Fig. 2 for the full SPC/E model,  $\Phi_{\text{pol}}$  should reach a plateau in the central bulk region, and GT water fails dramatically in this respect.

A self-consistent solution of Eq. (7) yields a very accu-

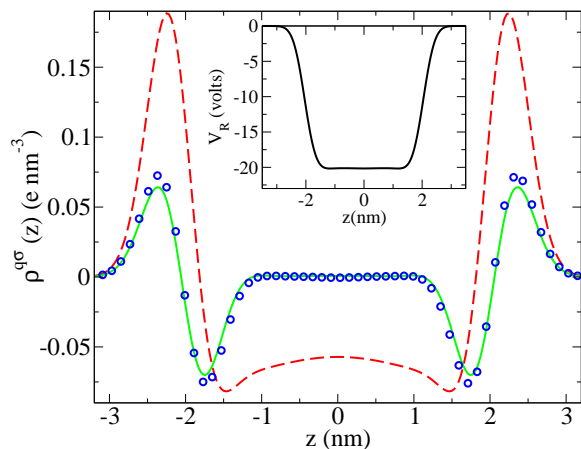


FIG. 3. Gaussian-smoothed charge densities with  $\sigma = 0.45$  nm. Labels are the same as in Fig. 2. The inset gives the effective field  $V_R(\mathbf{r})$ . Note that the bare  $V(\mathbf{r}) = 0$  in this case.

rate charge density that corrects all such failures. The inset in Fig. 3 gives the converged  $V_R(z)$ . Gaussian smoothing of the bare charge density as dictated by LMF theory averages over the simulation noise and local structure and reveals the much smaller coherent long-wavelength features that control the electrostatics [5]. The smoothed charge density quickly decays to a neutral bulk in Fig. 3 for both SPC/E water and LMF theory, while a true bulk never forms in GT water, causing the very poor polarization potential in Fig. 2.

These results highlight the advantages of the new LR-LMF method. It reduced the simulation time by more than an order of magnitude compared to use of the standard iteration method [5] or to use of the slab-corrected Ewald 3D method [14]. When using the standard iteration method, it proved very difficult to distinguish between equilibrium charge density fluctuations, present for any given field, and the desired changes in the charge density as the iteration proceeded to self-consistency. To obtain convergence, earlier workers had to use a large value of  $\sigma = 0.6$  nm and the charge density at each iteration was taken as the average over a set of 10 parallel simulations with different initial conditions [5].

In contrast, the results in Figs. 2 and 3 were obtained from only two very short trial simulations [11], starting first with the SCA  $V_0 = 0$ , and using the smaller bulk  $\sigma = 4.5$  nm. As before, the EXP form (3) was very noisy when used with SCA configurations, but the LR form (4) was much better behaved. It generated a second trial field in the linear regime that was virtually identical to the final self-consistent field shown in the inset of Fig. (3). The remaining effects of equilibrium fluctuations in the mimic system show up as small variations (about the size of the circle symbol) in the bulk value of the polarization potential in Fig. 2 or the heights of the charge density peaks in Fig. 3. As shown in the supplementary material,

excellent results have also been obtained for ion pairing in ionic solution models using the LR-LMF method [11].

Reaction field (RF) truncations of Coulomb interactions have recently been used in massively-parallel simulations of biological systems to permit much faster simulations [6]. LR-LMF theory may provide a promising linear-scaling alternative in which the effective field corrects known problems like those illustrated in Fig. 2 arising from simple RF or SCA truncations. More generally, we believe the efficient solutions generated by the LR-LMF method establish the full power of the basic mean field picture for both quantitative and qualitative analysis of a wide range of electrostatic and dielectric phenomena in nonuniform liquids.

This work was supported by the National Science Foundation (grants CHE0628178 and CHE0848574). We are grateful to Gerhard Hummer, Chris Jarzynski, and Jocelyn Rodgers for very helpful remarks.

---

\* Present address: State Key Laboratory of Supramolecular Structure and Materials, Jilin University, Changchun 130012, China

- [1] See, *e.g.*, L.P. Kadanoff, *Statistical Physics* (World Scientific, Singapore, 2000), pp. 209-246.
- [2] J.D. Weeks, K. Katsov, and K. Vollmayr, *Phys. Rev. Lett.* **81**, 4400 (1998); K. Katsov and J. D. Weeks, *J. Phys. Chem. B* **105**, 6738 (2001).
- [3] J.D. Weeks, *Ann. Rev. Phys. Chem.* **53**, 533 (2002).
- [4] Y.-G. Chen, C. Kaur, and J.D. Weeks, *J. Phys. Chem. B* **108**, 19874 (2004); J. M. Rodgers, C. Kaur, Y.-G. Chen and J. D. Weeks, *Phys. Rev. Lett.* **97**, 097801 (2006).
- [5] J. M. Rodgers and J. D. Weeks, *Proc. Nat. Acad. Sci. USA* **105**, 19136 (2008); J. M. Rodgers and J. D. Weeks, *J. Phys.: Cond. Matt.* **20**, 494206 (2008).
- [6] R. Schulz, B. Lindner, L. Petridis, and J.C. Smith, *J. Chem. Theory Comput.* **5**, 2798 (2009).
- [7] J.D. Weeks, D. Chandler, and H.C. Andersen, *J. Chem. Phys.* **54**, 5237 (1971).
- [8] A general field  $\phi(\mathbf{r})$  can be used in Eq. (1) as well.
- [9] See, *e.g.*, *Free Energy Calculations: Theory and Application in Chemistry and Biology*, edited by C. Chipot and A. Pohorille (Springer, Berlin, 2007).
- [10] D. M. Huang and D. Chandler, *Phys. Rev. E* **61**, 1501 (2000).
- [11] See EPAPS supplementary material at [URL to be inserted] for simulation details.
- [12] H.J.C. Berendsen, J.R. Grigera, and T.P. Straatsma, *J. Phys. Chem.* **91**, 6269 (1987).
- [13] C.Y. Lee, J.A. McCammon, and P.J. Rossky, *J. Chem. Phys.* **80**, 4448 (1984).
- [14] I.-C. Yeh and M. L. Berkowitz, *J. Chem. Phys.* **111**, 3155 (1999).
- [15] S. E. Feller, R. W. Pastor, A. Rojnuckarin, S. Bogusz, and B. R. Brooks, *J. Phys. Chem.* **100**, 17011 (1996).
- [16] E. Spohr, *J Chem Phys* **107**, 6342 (1997).

**Supplementary Material for:  
Efficient solutions of self-consistent mean field equations for dewetting and electrostatics in  
nonuniform liquids**

Zhonghan Hu\* and John D. Weeks

*Institute for Physical Science and Technology and Department of Chemistry and Biochemistry,  
University of Maryland, College Park, Maryland 20742*

---

\* Present address: State Key Laboratory of Supramolecular Structure and Materials, Jilin University, Changchun 130012, China



## I. SIMULATION DETAILS FOR DEWETTING OF THE LJ FLUID AROUND A HARD SPHERE SOLUTE AND FOR WATER CONFINED BETWEEN HYDROPHOBIC WALLS

In the following, equation and figure numbers refer to the main paper, unless otherwise indicated. Our Monte Carlo (MC) simulation for  $N = 2363$  LJ particles with a hard sphere solute at a state near the triple point with  $T = 0.85$  and  $\rho^B = 0.70$  follows the work of Huang and Chandler [1]. Configurations of a short trial simulation of 10000 MC steps based on the SCA and Eq. (4) were used in the LMF Eq. (1) to generate the trial field given by the solid line in Fig. (1b). A second trial simulation of 20000 steps using that field generated the final self-consistent LMF. Both runs were much shorter than the final production run of 200000 steps needed to determine the smooth profile of the full LJ system given by the circles in Fig. (1a).

Our molecular dynamics (MD) simulation of SPC/E water confined between hydrophobic LJ walls used the same system parameters and a modified DLPOLY2.18 MD package [2] similar to that described in detail in [3], with further modifications to save configurations needed for the LR-LMF theory. Two trial simulations with  $\sigma = 4.5$  nm each of 1 ns length and starting from the SCA were used to generate the data in Figs. (2) and (3). This was more than an order of magnitude faster than analogous results obtained using the standard iteration method [3]. Moreover, as discussed in detail in [4], a large value of  $\sigma = 0.6$  nm had to be used in the standard iteration method, because of problems in distinguishing equilibrium charge density fluctuations with a given estimate for the effective field from the desired iterative changes in the charge density. Even after averaging over results of 10 parallel simulations for each iteration, convergence was not found with  $\sigma = 4.5$  nm.

In contrast, the LR-LMF method uses the same set of equilibrium trial system configurations to determine the remaining changes in the charge density as self-consistency is achieved by iterating the LMF equation. Convergence was found using the same  $\sigma = 4.5$  nm used for the bulk, and required only two short trial simulations.

## II. CASE STUDY OF DILUTE IONIC SYSTEM

To further illustrate the versatility of the LR-LMF method we discuss here results for a dilute bulk ionic system at moderately strong coupling. This presents a challenge to theory, since the coupling is strong enough that traditional methods based on Poisson-Boltzmann theory will fail, but weak enough that the SCA alone will not be accurate unless a very large  $\sigma$  is used. Indeed, previous applications of LMF theory to bulk ionic solution models considered only strong-coupling states and used such a large  $\sigma$  that the SCA alone was accurate [5]. The present calculation represents the first self-consistent solution of the full LMF equation for a general ionic solution model in this difficult regime. As we will see only a single simulation in this case is needed to achieve full self-consistency.

The system is a size-asymmetric primitive model consisting of charged LJ molecules. The LJ interaction parameters are  $\sigma_+ = 4.0\text{\AA}$ ,  $\sigma_- = 3.0\text{\AA}$ ,  $\sigma_{+-} = 3.5\text{\AA}$ ,  $\varepsilon_+ = 0.1\text{kcal/mol}$ ,  $\varepsilon_- = 0.4\text{kcal/mol}$  and  $\varepsilon_{+-} = 0.2\text{kcal/mol}$ . The cation and anion has unit charge and mass of 12 and 30 respectively. The cutoff distance for both the LJ and Ewald short ranged interaction in the system is  $15\text{\AA}$ . The system has 1024 pairs of ions in a cubic box of size  $62\text{\AA}$  with  $T = 5000$  K. The MD simulation of the full system using Ewald sums used 90000 steps.

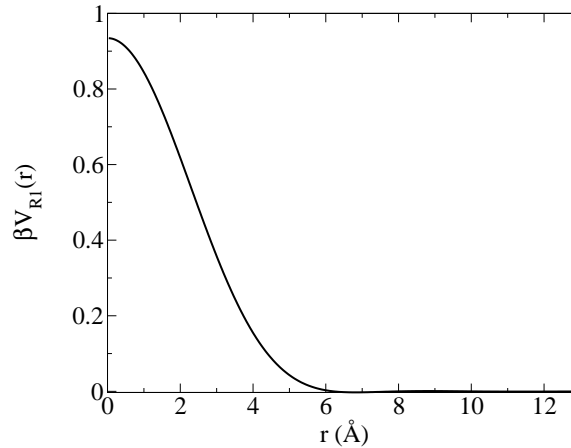


FIG. 1. The restructured field with a cation fixed at the origin

Results of MD simulations for the full system and for the LR-LMF method using the SCA as the trial system are presented here. Fig. (1) shows the restructured field with a cation fixed at the origin. The charge density around the cation is shown in Fig. (2). LR-LMF and EXP-LMF results overlap starting from SCA configurations and we show only the former in the graphs. Significant ion pairing is indicated by the strong first peak in the cation-anion correlation function in Fig. (3). The SCA

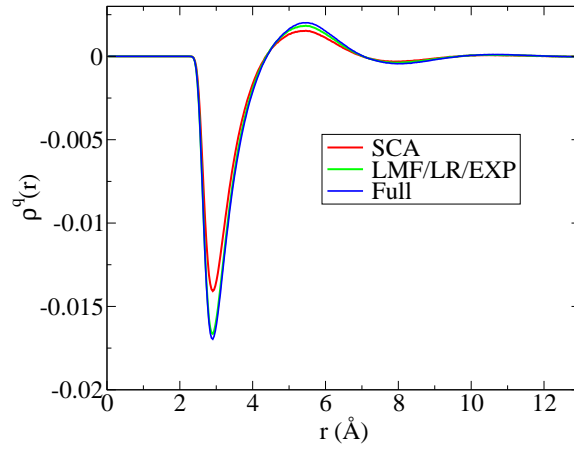


FIG. 2. The charge density around a cation

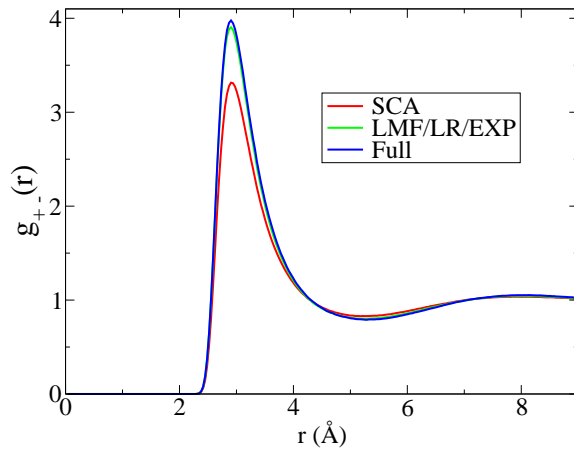


FIG. 3. The cation-anion correlation function

simulation used  $\sigma = 3.5\text{\AA}$ , a value for which the SCA correlation function had noticeable errors, as seen in Fig. (3). However the trial system based on SCA configurations is in the linear regime, and no further simulations are needed to get the converged results shown here from iteration of the LMF equation.

As explained in [6], it is useful to rewrite the LMF equation in a more numerically stable form for iteration so that small errors in the decay of the charge density are not amplified when convoluted with the long-ranged  $v_1$ . We used the specific method described in Appendix E of [4].

It is gratifying that LR-LMF theory allows for such accurate results using a small value of  $\sigma$ , since this permits fast mimic system simulations. However, care must be taken, since the underlying LMF theory itself will fail if too small a  $\sigma$  is used, and the small differences still visible for the LR-LMF and full correlation functions suggests we are close to the minimum accurate value.

- 
- [1] D. M. Huang and D. Chandler, Phys. Rev. E **61**, 1501 (2000).
  - [2] W. Smith, C. Yong, and P. Rodger, Molec. Sim. **28**, 385 (2002).
  - [3] J. M. Rodgers and J. D. Weeks, Proc. Nat. Acad. Sci. USA **105**, 19136 (2008).
  - [4] J.M. Rodgers, *Ph. D. Thesis*, University of Maryland, pp. 166-173 (2008).
  - [5] Y.-G. Chen and J. D. Weeks, Proc. Nat. Acad. Sci. USA **103**, 7560 (2006).
  - [6] Y.-G. Chen, C. Kaur, and J.D. Weeks, J. Phys. Chem. B **108**, 19874 (2004).